

# Correlating Structure and $KA^2$ Catalytic Activity of $Zn^{II}$ Hydrazone Complexes

Temiloluwa T. Adejumo,<sup>[a]</sup> Marianna Danopoulou,<sup>[b]</sup> Leandros P. Zorba,<sup>[b]</sup> Andrej Pevec,<sup>[c]</sup> Matija Zlatar,<sup>[d]</sup> Dušanka Radanović,<sup>[d]</sup> Milica Savić,<sup>[d]</sup> Maja Gruden,<sup>[a]</sup> Katarina K. Anđelković,<sup>[a]</sup> Iztok Turel,<sup>\*,[c]</sup> Božidar Čobeljić,<sup>\*,[a]</sup> and Georgios C. Vougioukalakis<sup>\*,[b]</sup>

Two new  $Zn(II)$  complexes bearing tridentate hydrazone-based ligands with NNO or NNS donor atoms were synthesised and characterised by elemental analysis, infrared (IR) and nuclear magnetic resonance (NMR) spectroscopies, and single crystal X-ray diffraction methods. These complexes, together with four previously synthesised analogues, having hydrazone ligands with a NNO donor set of atoms, were successfully employed as

catalysts in the ketone-amine-alkyne ( $KA^2$ ) coupling reaction, furnishing tetrasubstituted propargylamines, compounds with unique applications in organic chemistry. DFT calculations at the CAM-B3LYP/TZP level of theory were performed to elucidate the electronic structure of the investigated  $Zn(II)$  complexes, excellently correlating the structure of the complexes to their catalytic reactivity.

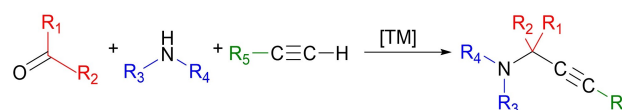
## Introduction

$Zn^{II}$  complexes with hydrazone ligands bearing a NNO or NNS donor set of atoms have been the subject of studies over many years for their applications in diverse fields.<sup>[1–6]</sup> Deprotonation of the  $-NH$  group results in the formation of keto-enol tautomerism ( $=N-N^--C=X$  or  $=N-N=C-X^-$ ) and can create a different tridentate NNX donor modes ( $X=O, S$ ).<sup>[7–11]</sup>  $Zn^{II}$  has the ability to form complexes with different coordination numbers and different types of geometries, while the flexibility of this type of multidentate-ligands allows these complexes to act as good catalysts in many catalytic organic transformations.<sup>[12]</sup> Com-

plexes encompassing NNX tridentate carbazone ligands form different types of coordination geometries. The geometry of pentacoordinated zinc(II) can be distorted trigonal bipyramidal,<sup>[13–19]</sup> distorted square pyramidal,<sup>[20–26]</sup> or somewhere between trigonal bipyramidal and square pyramidal.<sup>[27–29]</sup> Similarly, binuclear zinc(II) complexes of coordination number five with two acetate bridging ligands, in which three coordination sites are occupied by the NNS donor set of atoms, can have a trigonal bipyramidal or square pyramidal geometry. The analysis of previously synthesised ligands with NNO or NNS chromophores and their pentacoordinated  $Zn^{II}$  complexes lead to the conclusion that their catalytic properties are insufficiently investigated, and only in a few cases a detailed catalytic evaluation has been performed.<sup>[30,31]</sup>

On a different note, propargylamines are an important class of organic scaffolds, which can be exploited as precursors in the synthesis of nitrogen-containing compounds with high biological relevance. Tetrasubstituted propargylamines include the least studied family of propargylamines, which makes them particularly attractive for research.<sup>[32,33]</sup> These compounds are obtained *via* a three-step, one-pot reaction involving a ketone, an amine, and a terminal alkyne, in the presence of a transition metal catalyst (Scheme 1).<sup>[34]</sup>

The first transition metals utilized in the  $KA^2$  reaction as catalysts were Au<sup>[35]</sup> and Cu.<sup>[34,36]</sup> Recently, sustainable and low cost  $Zn^{II}$ <sup>[37]</sup> and  $Mn^{II}$ <sup>[38]</sup> salts were also successfully utilized by some of us. In a previous work, we established a new, bench-stable  $Zn^{II}$ -hydrazone complex supported by a NNO-donor hydrazone ligand, able to efficiently catalyse the  $KA^2$  coupling reaction, affording the desired propargylamines in good



Scheme 1.  $KA^2$  multicomponent coupling reaction.

[a] T. T. Adejumo, Prof. Dr. M. Gruden, Prof. Dr. K. K. Anđelković, Dr. B. Čobeljić  
Department of General and Inorganic Chemistry  
University of Belgrade – Faculty of Chemistry  
Studentski trg 12–16, 11000 Belgrade (Serbia)  
E-mail: bozidar@chem.bg.ac.rs

[b] M. Danopoulou, L. P. Zorba, Prof. Dr. G. C. Vougioukalakis  
Laboratory of Organic Chemistry, Department of Chemistry  
National and Kapodistrian University of Athens  
Panepistimiopolis, 15771 Athens (Greece)  
E-mail: vougiouk@chem.uoa.gr

[c] Dr. A. Pevec, Prof. Dr. I. Turel  
Department of Chemistry and Biochemistry  
Faculty of Chemistry and Chemical Technology  
University of Ljubljana  
Večna pot 113, 1000 Ljubljana (Slovenia)  
E-mail: Iztok.Turel@fkkt.uni-lj.si

[d] Dr. M. Zlatar, Dr. D. Radanović, M. Savić  
University of Belgrade – Institute of chemistry, technology and metallurgy  
Department of chemistry  
Njegoševa 12, P.O. Box 815, 11001 Belgrade (Serbia)

Supporting information for this article is available on the WWW under <https://doi.org/10.1002/ejic.202300193>

© 2023 The Authors. European Journal of Inorganic Chemistry published by Wiley-VCH GmbH. This is an open access article under the terms of the Creative Commons Attribution Non-Commercial NoDerivs License, which permits use and distribution in any medium, provided the original work is properly cited, the use is non-commercial and no modifications or adaptations are made.

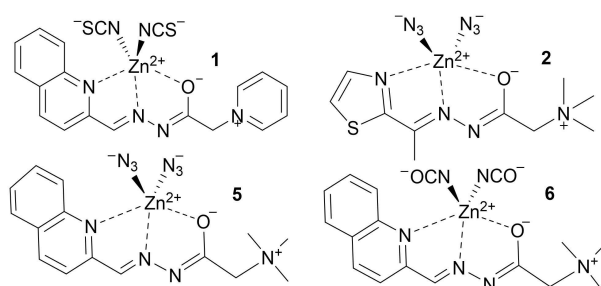
yields.<sup>[30]</sup> Encouraged by these studies, we set out to more extensively and systematically investigate the catalytic properties of zinc(II) hydrazone complexes. In this work, we synthesised and studied the catalytic activity of two new (**3** and **4**, vide infra) and four previously prepared Zn<sup>II</sup> complexes (**1**, **2**, **5** and **6**, Scheme 2).<sup>[24,25,27]</sup> The experimental studies on the catalytic activity of these Zn<sup>II</sup> complex is accompanied by thorough density functional theory (DFT) calculations. CAM-B3LYP/TZP level of theory was used to describe the electronic structures and molecular properties of the compounds of interest. Finite difference linearization (FDL) and frontier molecular orbital (FMO) approaches were used to determine the electronic chemical potential,  $\mu$ , the molecular hardness,  $\eta$ , the molecular softness,  $S$ , and the electrophilicity index  $\omega$ .

## Results and Discussion

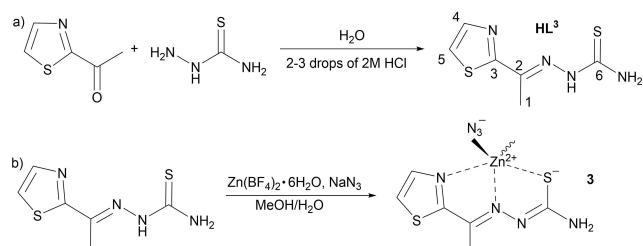
### Synthesis

The ligand (*E*)-2-(1-(thiazol-2-yl)ethylidene)hydrazine-1-carbothioamide (**HL<sup>3</sup>**) was obtained from the condensation of 2-acetylthiazole and thiosemicarbazide (Scheme 3a). Upon reacting **HL<sup>3</sup>** with Zn(BF<sub>4</sub>)<sub>2</sub>·6H<sub>2</sub>O and NaN<sub>3</sub> in a solvent mixture of water/methanol, mononuclear Zn<sup>II</sup> complex **3** with the composition [ZnL<sup>3</sup>(N<sub>3</sub>)<sub>n</sub>] was obtained (Scheme 3b). In complex **3**, Zn<sup>II</sup> is pentacoordinated with the thiazole nitrogen, the azomethine nitrogen, and thiolate sulfur atoms from the deprotonated hydrazone ligand, as well as with two azido ligands which are acting as bridging ligands.

The hydrazone ligand (*E*)-1-(2-oxo-2-(2-(1-(pyridin-2-yl)ethylidene)hydrazinyl)ethyl)-pyridine-1-ium chloride (**HL<sup>4</sup>Cl**)



Scheme 2. Structures of previously published Zn<sup>II</sup> complexes (**1**, **2**, **5** and **6**).<sup>[24,25,27]</sup>



Scheme 3. a) Synthesis of **HL<sup>3</sup>** ligand and b) [ZnL<sup>3</sup>(N<sub>3</sub>)<sub>n</sub>] complex (**3**).

was obtained from the condensation reaction of 2-acetylpyridine and Girard's P reagent (Scheme 4a). Reaction of **HL<sup>4</sup>Cl** with Zn(BF<sub>4</sub>)<sub>2</sub>·6H<sub>2</sub>O and NaN<sub>3</sub>, in a mixture of acetonitrile/water/methanol, gives mononuclear Zn<sup>II</sup> complex **4** with the composition [ZnL<sup>4</sup>(N<sub>3</sub>)<sub>2</sub>] (Scheme 4b). In complex **4**, the ligand is coordinated in its deprotonated, formally neutral, zwitterionic form to Zn<sup>II</sup> ion through the pyridine nitrogen, the imine nitrogen, and the carbonyl oxygen atoms, forming a pentacoordinated complex.

### IR spectra

The IR spectrum of [ZnL<sup>3</sup>(N<sub>3</sub>)<sub>n</sub>] (**3**) confirms coordination of the **HL<sup>3</sup>** ligand in its deprotonated form, given that the  $\nu(\text{N-H})$  band at 3435 cm<sup>-1</sup> is absent. Bands at 1464 and 892 cm<sup>-1</sup> in the IR spectrum of **3** correspond to  $\nu(\text{C=S}) + \nu(\text{C=N})$  and  $\nu(\text{C=S}) + \gamma(\text{CH})$ , respectively, while in the spectrum of non-coordinated **HL<sup>3</sup>** ligand  $\nu(\text{C=S}) + \nu(\text{C=N})$  and  $\nu(\text{C=S}) + \gamma(\text{CH})$  bands appear at 1481 and 1068 cm<sup>-1</sup>.

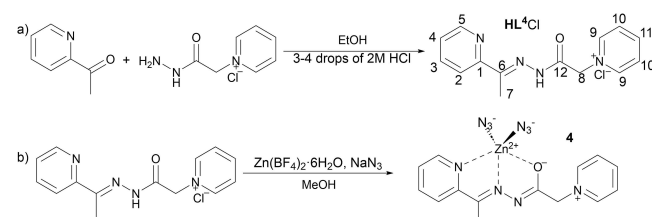
The vibration band originating from the NH moiety at 3425 cm<sup>-1</sup> in the IR spectrum of the **HL<sup>4</sup>Cl** ligand is absent in the spectrum of complex **4** [ZnL<sup>4</sup>(N<sub>3</sub>)<sub>2</sub>], confirming coordination of the ligand in its deprotonated form. Bands at 1462 and 892 cm<sup>-1</sup> in the IR spectrum of complex **4** correspond to  $\nu(\text{C=O}) + \nu(\text{C=N})$  and  $\nu(\text{C=O}) + \gamma(\text{CH})$ , respectively, while in the spectrum of non-coordinated **HL<sup>4</sup>Cl** ligand  $\nu(\text{C=O}) + \nu(\text{C=N})$  and  $\nu(\text{C=O}) + \gamma(\text{CH})$  bands appear at 1485 and 1068 cm<sup>-1</sup>.

In the IR spectra of **3** and **4** strong bands at 2084 cm<sup>-1</sup> and 2079 cm<sup>-1</sup>, respectively, correspond to the vibration of coordinated azido ligands.

In the IR spectrum of complex **4**, a band at 1629 cm<sup>-1</sup> corresponding to the  $\nu(\text{-O-C=N})$  vibration of the deprotonated  $\alpha$ -oxyazine form of ligand appears, instead of the carbonyl group band of non-coordinated **HL<sup>4</sup>Cl** at 1699 cm<sup>-1</sup>. The coordination of azomethine nitrogen imposes a shift of the  $\nu(\text{C=N})$  vibration from 1630 cm<sup>-1</sup> in the spectrum of **HL<sup>4</sup>Cl** to 1595 cm<sup>-1</sup> in the spectrum of complex **4**.

### NMR spectra

The presence of the NH signal in the <sup>1</sup>H NMR spectrum of ligand **HL<sup>3</sup>** at 10.6 ppm was not observed in the <sup>1</sup>H NMR spectrum of complex **3**, suggesting that the ligand **HL<sup>3</sup>** is coordinated in its deprotonated form **L<sup>3</sup>**. In the <sup>13</sup>C NMR spectrum it was observed



Scheme 4. a) Synthesis of the **HL<sup>4</sup>Cl** ligand and b) [ZnL<sup>4</sup>(N<sub>3</sub>)<sub>2</sub>] complex (**4**).

that complex **3** coordination sites are the thiazole nitrogen, the azomethine nitrogen, and the thiolate sulfur atoms. The downfield shift of the thiolate carbon (C6) from 179.4 ppm in the spectrum of **HL**<sup>3</sup> to 181.6 ppm in the spectrum of **3**, suggests coordination of the thiolate sulfur atom. The signal of the azomethine carbon atom (C2) at 144.7 ppm in the spectrum of the ligand is shifted upfield, in comparison to the spectrum of complex **3**, where it resonates at 138.9 ppm. From the <sup>1</sup>H NMR spectrum of complex **4** it can be deduced that the ligand **HL**<sup>4</sup>Cl is also coordinated in its deprotonated form, as the signal from the NH group at 11.5 ppm is absent. Coordination of **HL**<sup>4</sup>Cl through the oxygen atom of the carbonyl moiety results in upfield shift of signals of methylene C8–H protons from 6.1 ppm to 5.4 ppm in the spectrum of complex **4**. In the <sup>13</sup>C NMR spectrum of **HL**<sup>4</sup>Cl, C1 carbon resonates at 154.9 ppm, whereas the same carbon in complex **4** is observed at 149.3 ppm. Coordination of **HL**<sup>4</sup>Cl through the nitrogen atom of the azomethine group results in a downfield shift of the signal of C6, from 150.9 ppm to 161.3 ppm in the spectrum of complex **4**. Coordination of the carbonyl oxygen results in a downfield shift of C12 from 168.1 ppm in the spectrum of **HL**<sup>4</sup>Cl to 172.5 ppm in the spectrum of complex **4**.

### Crystal structures of [ZnL<sup>3</sup>(N<sub>3</sub>)<sub>n</sub>] (**3**) and [ZnL<sup>4</sup>(N<sub>3</sub>)<sub>2</sub>] (**4**) complexes

Complex **3** crystallises in the monoclinic crystal system with space group No.14 (*P*<sub>2</sub>/*c* cell setting). The unit cell of **3** contains four [ZnL<sup>3</sup>(N<sub>3</sub>)<sub>n</sub>] asymmetric units. In complex **3**, the Zn<sup>II</sup> site shows a distorted geometry, almost midway between the square pyramid and trigonal bipyramid, established on the basis of a calculated  $\tau_5$  parameter of 0.46 (Table S1 in the Supplementary material). Zn<sup>II</sup> is coordinated by NNS-set of

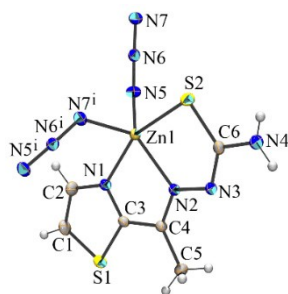


**Figure 1.** Coordination environment of Zn<sup>II</sup> in complex **3**. Thermal ellipsoids are drawn at the 30% probability level.

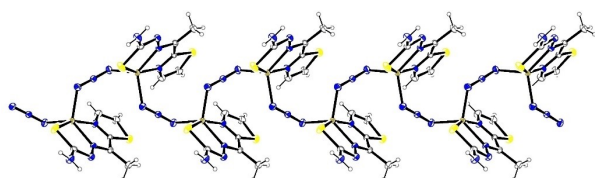


**Figure 2.** Zigzag polymeric chain generated by the  $\mu_{1,3}$  bridging function of the azide anions in complex **3**.

donor atoms of L<sup>3</sup> and two nitrogen atoms (N5 and N7<sup>i</sup> where  $i = x, \frac{1}{2} - y, -1/2 + z$ ) from symmetry related azide anions. The coordination environment of Zn<sup>II</sup> ion in **3** is depicted in Figure 1. The bond lengths and valence angles of complexes **3** and **4** are listed in Table S2.

The azide anions bridge Zn<sup>II</sup> ions in a  $\mu_{1,3}$  fashion so as to generate zigzag polymeric chains extending parallel with the *c* crystallographic axis (Figure 2). Further, the zigzag polymeric chains are assembled into a 3D network via hydrogen bonds involving terminal NH<sub>2</sub> group, thioamide nitrogen and one azide nitrogen (Table S3). The tridentate coordination of L<sup>3</sup> implies the formation of two fused five-membered chelate rings Zn–N–C–C–N and Zn–N–N–C–S, which are almost co-planar, as indicated by the dihedral angle of 2.2°. The Zn–L bond lengths (Zn–N<sub>Ar</sub> 2.1390(18) Å, Zn–S<sub>thiolate</sub> 2.3516(6) and Zn–N<sub>imine</sub> 2.1231(18) Å) observed in **3** fit into the range of values 2.125(4)–2.227(3), 2.324(2)–2.431(6) and 2.03(2)–2.156(4) Å, respectively, observed for the five-coordinate Zn<sup>II</sup> complexes with related tridentate NNS hydrazone-based ligands.<sup>[26–28,39–46]</sup> The azido ligands are coordinated to the Zn<sup>II</sup> in the bent mode, with N–N–Zn angles of 115.62(16) and 123.08(17)°.

Complex **4** crystallises in the same space group as complex **3**, with four neutral [ZnL<sup>4</sup>(N<sub>3</sub>)<sub>2</sub>] complex molecules in the unit cell. The molecular structure of [ZnL<sup>4</sup>(N<sub>3</sub>)<sub>2</sub>] with the atom numbering scheme is shown in Figure 3. In complex **4**, the Zn<sup>II</sup> ion has fivefold coordination with NNO-set of donor atoms of L<sup>4</sup> and two nitrogen atoms (N5 and N8) from the azido ligands. The calculated  $\tau_5$  value of 0.08 for [ZnL<sup>4</sup>(N<sub>3</sub>)<sub>2</sub>] indicates that the five-coordinate geometry of the Zn<sup>II</sup> ion is slightly distorted square pyramidal. The dihedral angle of 9.2° between two five-membered chelate rings (Zn–N–C–C–N and Zn–N–N–C–O) shows the non-coplanar nature of the metal–ligand system in **4**. The Zn–L bond lengths (Zn–N<sub>py</sub> 2.1759(18) Å, Zn–N<sub>imine</sub> 2.0430(19) Å and Zn–O<sub>enolate</sub> 2.2401(16) Å) observed in **4** are comparable with those found in five-coordinate Zn<sup>II</sup> complexes with related tridentate NNO hydrazone-based ligands. (2.08(3)–2.219(9), 2.044(2)–2.088(6) and 2.079(8)–2.21(2) Å,<sup>[13,18,47–51]</sup> respectively), although in complex **4** the Zn–O<sub>enolate</sub> bond is somewhat longer. The bond angles N6–N5–Zn1 and N9–N8–Zn1 of 128.9(2)° and 134.8(3)° suggest the bent coordination mode of the azide anions. In the crystals of **4**, the complex molecules [ZnL<sup>4</sup>(N<sub>3</sub>)<sub>2</sub>] are assembled into 3D supramolecular structure by

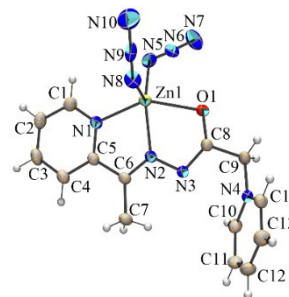


**Figure 3.** ORTEP<sup>[52]</sup> representation of the [ZnL<sup>4</sup>(N<sub>3</sub>)<sub>2</sub>] (**4**) complex. Thermal ellipsoids are drawn at the 30% probability level.

means of weak intermolecular C–H...N and C–H...O hydrogen bonds (Table S4).

A geometrical analysis of five-coordinate Zn<sup>II</sup> complexes with tridentate NNS and/or NNO hydrazone-based ligands was based on a Cambridge Structural Database (CSD)<sup>[53]</sup> search and on X-ray data for **3** and **4** reported herein. The survey of the Cambridge Structural Database revealed 30 structures of five-coordinate Zn<sup>II</sup> complexes with NNS and 50 structures with NNO hydrazone-based ligands; the other two coordination sites being occupied by monodentate ligands. Details of CSD search are given in the Supplementary material together with the angular structural parameters ( $\tau_5$ ) calculated for the corresponding complexes (Table S1). The geometric parameters have been calculated using the crystallographic program PLATON.<sup>[54]</sup> On the basis of the calculated  $\tau_5$  values, it can be concluded that the geometry of five-coordinate Zn<sup>II</sup> complexes with NNS hydrazone-based ligands varies from perfect square pyramidal to distorted trigonal bipyramidal and for five-coordinate Zn<sup>II</sup> complexes with NNO hydrazone-based ligands from perfect square pyramidal to very distorted square pyramidal forms.

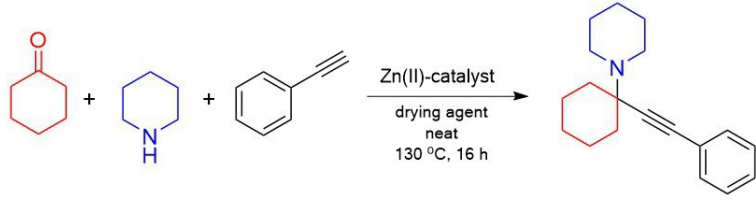
### Catalytic activity evaluation in the KA<sup>2</sup> coupling reaction

Cyclohexanone, piperidine, and phenylacetylene were chosen as model substrates to initially evaluate the catalytic activity of the Zn<sup>II</sup> hydrazone complexes in the KA<sup>2</sup> reaction.<sup>[33]</sup> By using 5 mol% of complex **2** as catalyst and MgSO<sub>4</sub> as drying reagent, the reaction proceeds smoothly, allowing the formation of the

desired propargylamine in 80% isolated yield (Entry 1, Table 1). It is well known that the KA<sup>2</sup> cross-coupling reaction releases water as the sole byproduct and, therefore, the use of a drying reagent is usually beneficial, improving the yield of the desired product.<sup>[33]</sup> Increasing the catalyst loading to 10 mol% resulted in a reduction of the isolated yield (Entry 2, Table 1). When the reaction was performed under open-air conditions, the desired propargylamine was isolated in 70% yield (Entry 3, Table 1). Using 0.5 equivalents of titanium ethoxide [Ti(OEt)<sub>4</sub>] as additive, along with a 5 mol% catalyst loading, led to an 86% isolated yield (Entry 4, Table 1). Titanium ethoxide is a Lewis acid, playing a dual role in promoting the reaction: On one hand, it exhibits a great water-scavenging ability that promotes the reaction by “protecting” the catalytic system, especially when this is relatively sensitive to the presence of water. On the other hand, Ti(OEt)<sub>4</sub> assists to overcome the low reactivity of ketones, by coordinating with their carbonyl group, thus improving their reactivity towards the formation of the ketimine intermediate and, subsequently, the desired propargylamine formation.<sup>[55]</sup>

Increasing the amount of titanium ethoxide to 1 equivalent had a negative result on the reaction outcome (Entry 5, Table 1). Next, we evaluated the catalytic performance of Zn<sup>II</sup> complexes **1** and **3–6**, by adopting the optimised conditions developed for complex **2**, i.e. using 5 mol% catalyst loading and 0.5 equivalents of Ti(OEt)<sub>4</sub>. When complex **4** was used as the catalyst, it led to a 92% isolated yield of the desired propargylamine, exhibiting the highest reactivity among all

Table 1. Optimisation of the KA<sup>2</sup> reaction conditions.



Entry	Catalyst	Loading [mol%]	Additives (0.5 eq)	% Isolated Yield
1	<b>2</b>	5	MgSO <sub>4</sub>	80
2	<b>2</b>	10	MgSO <sub>4</sub>	62
3	<b>2</b>	5	MgSO <sub>4</sub>	70 <sup>[a]</sup>
4	<b>2</b>	5	Ti(OC <sub>2</sub> H <sub>5</sub> ) <sub>4</sub>	86
5	<b>2</b>	5	Ti(OC <sub>2</sub> H <sub>5</sub> ) <sub>4</sub>	82 <sup>[b]</sup>
6	<b>1</b>	5	Ti(OC <sub>2</sub> H <sub>5</sub> ) <sub>4</sub>	66
7	<b>3</b>	5	Ti(OC <sub>2</sub> H <sub>5</sub> ) <sub>4</sub>	63
8	<b>4</b>	5	<b>Ti(OC<sub>2</sub>H<sub>5</sub>)<sub>4</sub></b>	<b>92</b>
9	HL <sup>4</sup>	5	Ti(OC <sub>2</sub> H <sub>5</sub> ) <sub>4</sub>	Traces <sup>[c]</sup>
10	<b>5</b>	5	Ti(OC <sub>2</sub> H <sub>5</sub> ) <sub>4</sub>	56
11	<b>6</b>	5	Ti(OC <sub>2</sub> H <sub>5</sub> ) <sub>4</sub>	54
12	Zn(OAc) <sub>2</sub>	5	Ti(OC <sub>2</sub> H <sub>5</sub> ) <sub>4</sub>	30 <sup>[c]</sup>
13	–	–	Ti(OC <sub>2</sub> H <sub>5</sub> ) <sub>4</sub>	No reaction

All reactions were performed in a flame dried Schlenk under inert conditions on a 0.5 mmol scale. The drying reagent was added on 0.5 eq (0.25 mmol) scale unless otherwise noted. [a] The reaction was performed in open air. [b] Titanium(IV) ethoxide 1 eq. (0.5 mmol). [c] Detected by GC-MS analysis.

complexes tested (Entry 8, Table 1). Complexes **1** and **3** furnished the product in 66 and 63% yield (Entry 6 and 7, respectively, Table 1), while complexes **5** and **6** showed even lower catalytic performance, namely, 56% and 54%, respectively (Entry 10 and 11, Table 1). To confirm that the coordination of the ligand to the zinc center is responsible for the high catalytic activity of complex **4**, a reaction was set up employing 5 mol% of  $\text{Zn}(\text{OAc})_2$  as catalyst,<sup>[37,38]</sup> resulting in the formation of the desired product in a lower, 30% yield, as measured by GC–MS analysis. Traces of the propargylamine product were observed when  $\text{HL}^4\text{Cl}$  ligand was used alone, in the absence of a zinc source (Entry 9, Table 1), which is attributed to a very low yielding reaction due to the elevated temperature. A blank reaction was also set up, in the absence of complex **4** (Entry 13, Table 1), resulting in the retrieval of starting materials.

We then probed the reactivity of a number of substrates under the optimised conditions, by employing a variety of secondary amines, aliphatic ketones, and alkynes, obtaining the corresponding propargylamines in moderate to excellent yields. Compared to piperidine, morpholine exhibited reduced reactivity, allowing the formation of **4b** in 67% isolated yield (Table 2), which resembles the reactivity shown in the case of Zn-based ligand-free  $\text{KA}^2$  system,<sup>[33]</sup> whereas the challenging primary amine 1-octylamine and di-*n*-propylamine allowed the isolation of products **4c** and **4d** in 42% and 40% yield, respectively. The relatively low isolated yield of **4c** can be rationalised by the relatively high stability of the intermediate imine formed, whereas, in the case of **4d**, formation of an allene byproduct was also observed (Table 2).<sup>[56]</sup> *p*-Tolyl-acetylene and *p*-chloro-phenylacetylene furnished products **4e** and **4f** both in moderate yields, with pyrrolidine and cyclohexanone, despite the fact that the former bears an electron donating group at the *para* position. Reaction of cyclohexanone with *p*-methoxy-

phenylacetylene and piperidine afforded **4g** in 96% yield, which was anticipated, given that the alkyne employed is substituted with a strongly electron donating group at the *para* position, thus allowing an efficient nucleophilic attack of the zinc acetylide to the ketiminium cation. 1-Octyne allowed the isolation of **4h** in moderate yields (Table 2). Regarding the reactivity of ketones, reaction of 3-pentanone, phenylacetylene, and pyrrolidine allowed the formation of **4i** in 75% yield. Overall, complex **4** shows a very satisfactory catalytic efficiency in the  $\text{KA}^2$  reaction, also taking into account the current state of the art in the field.

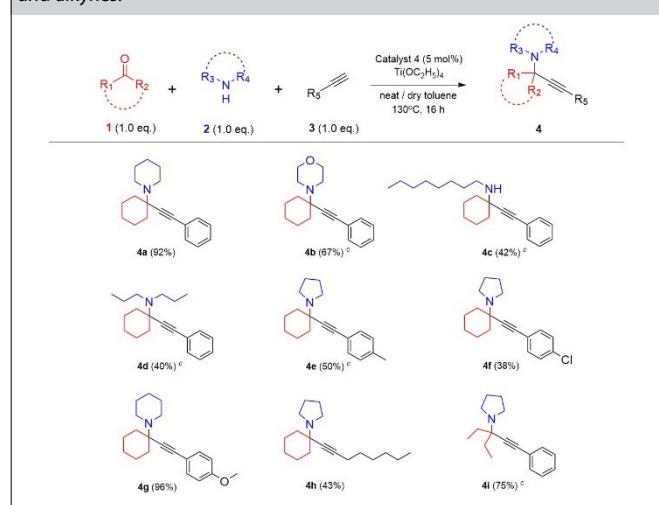
## Computational results

DFT calculations were performed to elucidate the electronic structure of investigated  $\text{Zn}^{\text{II}}$  complexes **1–6** and to correlate their structure with their reactivity. The X-ray determined structures of all complexes was used, and CAM-B3LYP/TZP level of theory was employed. In all complexes, the central  $\text{Zn}^{\text{II}}$  ion is coordinated with a tridentate Schiff base type ligand and two monodentate anions. Electrostatic potential surfaces of all six complexes are presented in Figure 4. Mapped surfaces are presented with a “divergent colormap”, with red and blue regions indicating negatively and positively charged areas, respectively. These maps illustrate the charge distributions in all six complexes. Negatively charged areas are, in all cases, concentrated around the monodentate anionic ligands. As expected, in complexes **1**, **2**, and **4–6**, positively charged regions are distributed mainly on the quaternary ammonium moiety.

Descriptors within the groundwork of Conceptual DFT<sup>[57,58]</sup> allow interpreting and predicting the reactivity of molecules.<sup>[30,59]</sup> The descriptors are intrinsic properties of a molecule directly obtained from DFT calculations.<sup>[60]</sup> In this work, we studied the electronic chemical potential,  $\mu$ , the molecular hardness,  $\eta$ , the molecular softness,  $S$ , and the electrophilicity index  $\omega$ .

These parameters are evaluated by two different approaches,<sup>[61]</sup> the finite difference linearisation (FDL) and the frontier molecular orbital (FMO) approaches:

**Table 2.** Substrate scope of the reaction with ketones, secondary amines and alkynes.<sup>[a,b]</sup>



[a] Isolated yields are shown in parenthesis. [b] Reaction conditions: catalyst (5 mol%), 0.5 mmol ketone, 0.5 mmol amine, 0.5 mmol alkyne, 0.25 mmol additive, neat (130 °C, 16 h). [c] Addition of 200  $\mu\text{L}$  dry toluene.

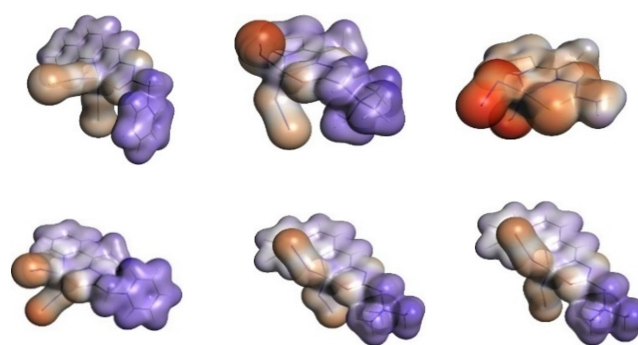


**Figure 4.** Electrostatic potential surfaces (at 0.01 au) of complexes **1–3** (up row) and **4–6** (down). Divergent color map from  $-0.20$  (red) to  $+0.21$  (blue) a.u. is used.

$$\mu = \frac{E_e(N+1) - E_e(N-1)}{2} \approx \frac{e_{HOMO} + e_{LUMO}}{2} \quad (1)$$

$$\eta = E_e(N+1) - 2E_e(N) + E_e(N-1) \approx e_{LUMO} - e_{HOMO} \quad (2)$$

$$S = \frac{1}{\eta} \quad (3)$$

$$\omega = \frac{\mu^2}{2\eta} \quad (4)$$

The FDL approach is based on the calculations of the electronic energy of a molecule studied and the molecule with one more and one less electron ( $N$ ,  $N+1$ , and  $N-1$  electron systems). The FMO approach is based on the Kohn-Sham orbital energies of the highest occupied MO and the lowest unoccupied one ( $e_{HOMO}$  and  $e_{LUMO}$ ). The negative value of chemical potential is related to the chemical stability of a molecule. Hardness and softness pertain to molecular reactivity. Molecules with a higher degree of softness are more polarizable and more reactive. On the contrary, hard molecules have lower polar-

izability, high kinetic stability, and low chemical reactivity. From the orbital point of view, a HOMO-LUMO gap is attributed to the molecular hardness [Eq. (2)].

The frontier molecular orbitals (HOMO, LUMO) of investigated complexes are shown in Figure 5. The HOMOs are localised at the monodentate anionic ligands, with slight delocalisation toward the metal center. In the case of 3, HOMO is on both azide ligands. HOMO of 2 and 4 is localized on a single azide ligand. For 1, 5, and 6, the delocalisation of HOMO within two monodentate ligands is asymmetric. LUMOs of 1 and 4 are localised on the pyridinium cationic part of the chelate ligands. LUMOs of other complexes are delocalised at tridentate ligands.

The conceptual DFT reactivity descriptors of complexes 1–6, evaluated at CAM-B3LYP/TZP level of theory, in both FDL and FMO approaches, are shown in Table 3. Complex 4 has the highest value of the molecular softness, i.e., it is the softest of the considered  $Zn^{II}$  complexes. Obviously [Eq. (3)], complex 4 has the lowest value of molecular hardness. Note that complex 4 is indeed the one showing the highest catalytic performance (Table 3).

The hardest of studied molecules is complex 6, also showing the lowest catalytic efficiency. The key descriptor for the reactivity of the herein studied complexes, i.e., for their catalytic activity, is molecular softness. There is a linear relationship between the molecular softness (Table 3) and the catalytic performance described by the % isolated yield of the desired propargylamine product (Table 1), as shown in Figure 6 ( $R^2 = 0.8900$ ). Thus, the higher the molecular softness of a complex, the more pronounced its catalytic efficiency.

Numerical values of descriptors obtained in FDL and FMO approaches are different, because they are estimated differently. Still, what is very important is that the trends are the same. There is a linear relationship between the two sets of data, as exemplified for  $\mu$ ,  $S$ , and  $\omega$ , in Figure 7 ( $R^2 = 0.9991$ ,  $R^2 = 0.9878$ ,  $R^2 = 0.9630$ , respectively). This justifies the common use of the simpler FMO approximation.

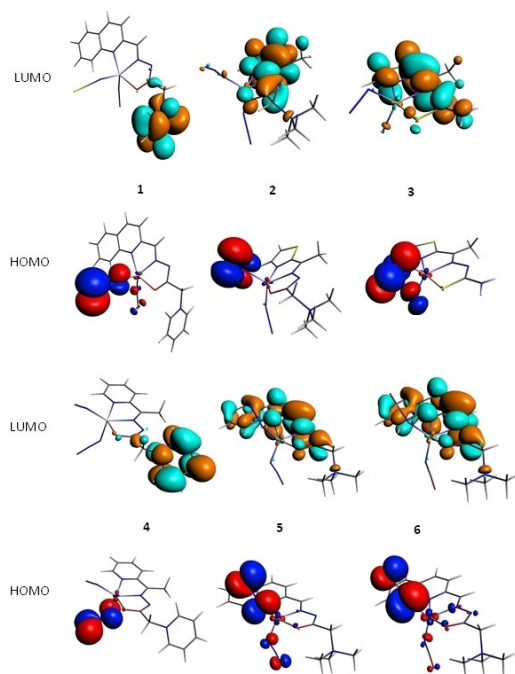
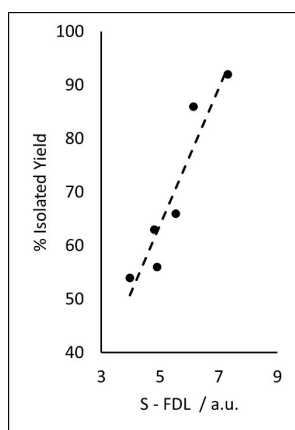


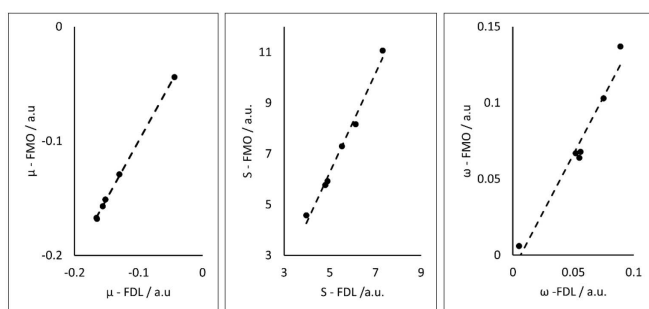
Figure 5. Frontier orbitals (HOMO, LUMO) of  $Zn^{II}$  complexes 1–6 (isosurfaces 0.03 a.u.).

Table 3. Conceptual DFT reactivity descriptors (in a.u.) of studied complexes 1–6. All descriptors are calculated using the X-ray geometries at the CAM-B3LYP/TZP level of theory based on finite difference linearisation (FDL) and frontier molecular orbital approximation (FMO).

		1	2	3	4	5	6
FDL	$\mu$	−0.165	−0.13	−0.044	−0.156	−0.152	−0.166
	$\eta$	0.181	0.163	0.208	0.137	0.204	0.252
	$S$	5.531	6.137	4.801	7.311	4.898	3.971
	$\omega$	0.075	0.052	0.005	0.089	0.056	0.055
FMO	$\mu$	−0.168	−0.129	−0.044	−0.157	−0.151	−0.167
	$\eta$	0.137	0.122	0.173	0.090	0.169	0.218
	$S$	7.305	8.165	5.777	11.074	5.926	4.579
	$\omega$	0.103	0.067	0.006	0.137	0.068	0.064



**Figure 6.** The linear relationship between the % isolated yield of the desired propargylamine product and the molecular softness ( $S$ ) calculated in the FDL approach at CAM-B3LYP/TZP level of theory.



**Figure 7.** The linear relationship between a) the electronic chemical potential,  $\mu$ , calculated with FMO and FDL approaches (left), b) the molecular softness,  $S$ , calculated with FMO and FDL approaches (middle), c) the electrophilicity index,  $\omega$ , calculated with FMO and FDL approaches (right).

## Conclusions

Upon reacting (*E*)-2-(1-(thiazol-2-yl)ethylidene)hydrazine-1-carbothioamide (**HL**<sup>3</sup>) with  $\text{Zn}(\text{BF}_4)_2 \cdot 6\text{H}_2\text{O}$  and  $\text{NaN}_3$ , complex **3** with the composition  $[\text{ZnL}^3(\text{N}_3)_n]$  was obtained. The geometry around  $\text{Zn}^{\text{II}}$  is distorted, between the square pyramid and trigonal bipyramid. The azide anions bridge  $\text{Zn}^{\text{II}}$  ions in a  $\mu_{1,3}$  fashion, so as to generate zigzag polymeric chains. The reaction of (*E*)-1-(2-oxo-2-(2-(1-(pyridin-2-yl)ethylidene)hydrazinyl)ethyl)pyridin-1-ium chloride (**HL**<sup>4</sup>Cl) with  $\text{Zn}(\text{BF}_4)_2 \cdot 6\text{H}_2\text{O}$  and  $\text{NaN}_3$  provides  $\text{Zn}^{\text{II}}$  complex **4** with composition  $[\text{ZnL}^4(\text{N}_3)_2]$ . The five-coordination geometry of the  $\text{Zn}^{\text{II}}$  ion is distorted square pyramidal. In both **3** and **4**, the tridentate ligand is coordinated in its deprotonated form to the  $\text{Zn}^{\text{II}}$  ion. In addition to complexes **3** and **4**, we also thoroughly studied, experimentally and theoretically, four previously synthesised  $\text{Zn}^{\text{II}}$  complexes: **1**, **2**, **5**, and **6**.

Evaluation of the catalytic properties of the  $\text{Zn}^{\text{II}}$  complexes in the  $\text{KA}^2$  reaction shows that the most active compound, when used as a catalyst, is complex **4**. It leads to a 92% isolated yield of the desired propargylamine product. Complexes **1** and **3** provide the product in 66% and 63% yield respectively, while

the least effective catalysts are complexes **5** and **6** (yields 56 and 54 %, respectively).

The catalytic activity results are in full agreement with the findings of the DFT calculations. Complex **4** shows the highest value of molecular softness and the lowest value of molecular hardness. The hardest molecule, among those studied herein, is complex **6**, with the poorest catalytic performance. This correlation, between experimental and theoretical results, is excellently visualised in the linear relationship between the isolated yield of the desired propargylamine product and the calculated molecular softness,  $S$ .

## Experimental Section

### Materials and Methods

2-Acetylpyridine ( $\geq 99\%$ ), thiosemicarbazide (99%), and  $\text{NaOCN}$  (96%) were obtained from Aldrich, 2-acetylthiazole (99%) from Acros Organics, Girard's T reagent (99%) from TCI, Girard's P reagent ( $>95\%$ ) from Fluorochem, 2-quinolinecarboxaldehyde (97%) from Alfa Aesar,  $\text{NaN}_3$  (99%) Riedel-de Haën, and  $\text{NH}_4\text{SCN}$  (99%) Zorka Šabac. All chemicals and reagents used for the catalytic evaluation experiments were purchased from Sigma-Aldrich, Fluorochem, Across Organics or Alfa-Aesar and were used without further purification, except for cyclohexanone, piperidine, pyrrolidine, and morpholine, which were purified by distillation prior to use. Toluene was dried based on standard literature procedures. IR spectra were recorded on a Nicolet 6700 Fourier transform infrared (FT-IR) spectrometer using the attenuated total reflectance (ATR) technique in the region  $4000\text{--}400\text{ cm}^{-1}$  (vs-very strong, s-strong, m-medium, w-weak, bs-broad signal).  $^1\text{H}$  and  $^{13}\text{C}$  NMR spectra were recorded on Varian 400/54 PS spectrometer ( $^1\text{H}$  at 400 MHz,  $^{13}\text{C}$  at 125 MHz) at room temperature using TMS as internal standard in  $\text{DMSO-}d_6$ . Chemical shifts are expressed in ppm ( $\delta$ ) values and coupling constants ( $J$ ) in Hz. Elemental analyses (C, H, N and S) were performed by standard micro-methods using the ELEMENTAR-Vario ELIII C.H.N.S.O analyser.

**Synthesis of ligand  $\text{HL}^1\text{Cl}$ :** The ligand  $\text{HL}^1\text{Cl}$  was synthesised by the reaction of 2-quinolinecarboxaldehyde and Girard's P reagent in ethanol according to the previously described method.<sup>[6]</sup> Elemental analysis calcd. for  $\text{C}_{17}\text{H}_{15}\text{N}_4\text{OCl}$ : C 62.48%, H 4.63%, N 17.15%; found: C 62.50%, H 4.65%, N 17.11%. IR (ATR,  $\text{cm}^{-1}$ ): 3418 (s), 3133 (s), 3065 (s), 2958 (s), 1695 (vs), 1487 (s), 1428 (w), 1389 (s), 1274 (s), 1125 (m), 773 (m), 750 (w).  $^1\text{H}$  NMR (400 MHz,  $\text{DMSO-}d_6$ ),  $\delta$  (ppm): 6.13 (s, 2H, C11-H), 7.64 (t, 1H, C6-H), 7.79 (t, 1H, C7-H), 8.01 (m, 2H, C5-H, C8-H), 8.12 (d, 1H, C3-H), 8.23 (t, 2H, C13-H), 8.32 (s, 1H, C9-H), 8.47 (d, 1H, C4-H), 8.69 (t, 1H, C14-H), 9.07 (d, 2H, C12-H).

**Synthesis of complex **1**:** Complex **1** was synthesised by the reaction of  $\text{HL}^1\text{Cl}$ ,  $\text{Zn}(\text{BF}_4)_2 \cdot 6\text{H}_2\text{O}$  and  $\text{NH}_4\text{SCN}$  in methanol according to the previously described method.<sup>[24]</sup> Elemental analysis calcd. for  $\text{C}_{19}\text{H}_{15}\text{N}_6\text{OS}_2\text{Zn}$ : C 48.26%, H 3.20%, N 17.75%, S 13.56%; found: C 48.30%, H 3.25%, N 17.68%, S 13.49%. IR (ATR,  $\text{cm}^{-1}$ ): 3060 (m), 2075 (vs), 1562 (m), 1518 (s), 1488 (s), 1433 (w), 1360 (m), 1271 (w), 1084 (m), 829 (w), 737 (w).  $^1\text{H}$  NMR (400 MHz,  $\text{DMSO-}d_6$ ),  $\delta$  (ppm): 5.60 (s, 2H, C11-H), 7.70 (t, 1H, C6-H), 7.85 (d, 1H, C3-H), 7.94 (t, 1H, C7-H), 8.09 (d, 1H, C5-H), 8.19 (t, 2H, C13-H), 8.24 (d, 1H, C8-H), 8.56 (s, 1H, C9-H), 8.65 (t, 1H, C14-H), 8.70 (d, 1H, C4-H), 9.12 (d, 2H, C12-H).

**Synthesis of ligand  $\text{HL}^2\text{Cl}$ :** The ligand  $\text{HL}^2\text{Cl}$  was synthesised by the reaction of Girard's reagent T and 2-acetylthiazole in water according to the previously described method.<sup>[30]</sup> Elemental analysis

calcd. for  $C_{10}H_{17}N_4OSCl$ : C 43.40%, H 6.19%, N 20.24%, S 11.58%; found: C 43.45%, H 6.21%, N 20.20%, S 11.52%. IR (ATR,  $cm^{-1}$ ): 3092 (m), 3018 (m), 2955 (s), 1702 (vs), 1550 (vs), 1487 (s), 1401 (m), 1201 (s), 1135 (w), 787 (w).  $^1H$  NMR (400 MHz, DMSO- $d_6$ ),  $\delta$  (ppm): 2.41 (s, 3H, C5-H), 3.30 (s, 9H, C8-H), 4.60 (s, 2H, C7-H), 4.82 (s, 2H, C7-H), 7.85 (d, 1H, C2-H), 7.93 (d, 1H, C3-H), 11.61 (s, 1H, N-H).

**Synthesis of complex 2:**  $Zn^{II}$  complex 2 was synthesised by the reaction of  $HL^2Cl$ ,  $Zn(BF_4)_2 \cdot 6H_2O$  and  $NaN_3$  in methanol according to the previously described method.<sup>[27]</sup> Elemental analysis calcd. for  $C_{10}H_{16}N_{10}OSZn$ : C 30.82%, H 4.14%, N 35.94%, S 8.23%; found: C 30.76%, H 4.18%, N 35.83%, S 8.21%. IR (ATR,  $cm^{-1}$ ): 3378 (w), 2057 (vs), 1600 (w), 1540 (s), 1481 (w), 1433 (w), 1407 (w), 1339 (m), 1285 (w), 1203 (w), 1153 (w), 1116 (w), 1079 (w), 880 (w).  $^1H$  NMR (400 MHz, DMSO- $d_6$ ),  $\delta$  (ppm): 2.53 (s, 3H, C5-H), 3.23 (s, 9H, C8-H), 4.13 (s, 2H, C7-H), 7.92 (d, 1H, C2-H), 8.04 (d, 1H, C3-H).

**Synthesis of ligand  $HL^3$ :** The ligand  $HL^3$  was synthesised by the reaction of 2-acetylthiazole (1.040 mL, 10 mmol) dissolved in water (20 ml) with solid thiosemicarbazide (0.911 g, 10 mmol) according to the previously described method (Scheme 3a).<sup>[60]</sup> Yield: 1.842 g (92%). IR (ATR,  $cm^{-1}$ ): 3435 (s), 3248 (s), 3188 (s), 3099 (m), 3071 (m), 2983 (m), 2065 (w), 1647 (w), 1589 (s), 1510 (s), 1482 (s), 1452 (m), 1425 (s), 1365 (m), 1282 (m), 1166 (m), 1107 (m), 1069 (m), 1039 (m), 958 (w), 881 (w), 847 (w), 755 (w), 712 (w), 638 (w). Elemental analysis calcd. for  $C_6H_8N_4S_2$ : C 35.98%, H 4.03%, N 27.98%, S 32.02%; found: C 35.84%, H 4.10%, N 27.89%, S 31.98%.  $^1H$  NMR (400 MHz, DMSO- $d_6$ ),  $\delta$  (ppm): 2.43 (s, 3H, C1-H), 7.80 (d, 1H, C4-H), 7.89 (d, 1H, C5-H), 7.69; 8.53 (s,  $NH_2$ ), 10.67 (s, 1H, NH).  $^{13}C$  NMR (125 MHz, DMSO- $d_6$ ),  $\delta$  (ppm): 14.1 (C1), 123.1 (C4), 144.7 (C2), 143.7 (C5), 167.5 (C3), 179.4 (C6).

**Synthesis of complex  $[ZnL^3(N_3)]_n$  (3):** The ligand  $HL^3$  (0.040 g, 0.20 mmol) was dissolved in solvent mixture of MeOH/ $H_2O$  (25/5 mL) and solid  $Zn(BF_4)_2 \cdot 6H_2O$  (0.069 g, 0.20 mmol) was added (Scheme 3b). After complete dissolution of  $Zn(BF_4)_2 \cdot 6H_2O$  in reaction mixture,  $NaN_3$  (0.052 g, 0.80 mmol) dissolved in water (5 mL) was added. The mixture was refluxed for 2 h. After slow evaporation of solvent at room temperature for one day, yellow crystals were obtained. Yield: 60 mg (87%). Elemental analysis calcd. for  $C_6H_7N_7S_2Zn$ : C 23.50%, H 2.30%, N 31.97%, S 20.91%; found: C 23.47%, H 2.33%, N 31.91%; S 20.87%. IR (ATR,  $cm^{-1}$ ): 3419 (s), 3399 (m), 3291 (m), 3227 (w), 3169 (m), 3104 (m), 3089 (m), 2084 (s), 2048 (s), 1997 (m), 1625 (s), 1585 (m), 1499 (m), 1428 (s), 1388 (s), 1369 (m), 1342 (m), 1301 (m), 1204 (m), 1167 (m), 1112 (m), 1035 (w), 998 (w), 886 (w), 790 (m), 746 (m), 684 (m), 643 (w), 596 (w), 495 (w), 472 (w).  $^1H$  NMR (400 MHz, DMSO- $d_6$ ),  $\delta$  (ppm): 2.38 (s, 3H, C1-H), 7.38 (s, 2H,  $NH_2$ ), 7.83 (d, 1H, C5-H), 7.89 (d, 1H, C4-H).  $^{13}C$  NMR (125 MHz, DMSO- $d_6$ ),  $\delta$  (ppm): 15.75 (C1), 123.18 (C4), 138.93 (C2), 142.27 (C5), 167.08 (C3), 181.61 (C6).

**Synthesis of ligand  $HL^4Cl$ :** 2-Acetylpyridine 0.363 g (3.00 mmol) and Girard's P reagent 0.563 g (3.00 mmol) were dissolved in ethanol (40 mL) and 1–2 drops of cc. HCl were added (Scheme 4a). The mixture was refluxed for 2 h. After cooling to the room temperature, a white precipitate was filtered and washed with ethanol. Yield: 0.451 g (52%). Elemental analysis calcd. for  $C_{14}H_{15}ClN_4O$ : C 57.83%, H 5.20%, N 19.27%; found: C 57.80%, H 5.23%, N 19.25%. IR (ATR,  $cm^{-1}$ ): 3425 (s), 3273 (m), 3125 (m), 3054 (s), 2949 (w), 1699 (vs), 1630 (s), 1582 (m), 1485 (vs), 1453 (m), 1433 (s), 1384 (s), 1323 (w), 1263 (s), 1221 (m), 1197 (m), 1150 (w), 1111 (m), 1081 (w), 848 (w), 790 (m), 774 (m), 725 (w), 702 (m), 646 (m), 600 (w), 569 (w).  $^1H$  NMR (400 MHz, DMSO- $d_6$ ),  $\delta$  (ppm): 2.37 (s, 3H, C7-H), 6.14 (s, 2H, C8-H), 7.41 (t, 1H, C4-H), 7.85 (t, 1H, C3-H), 8.13 (d, 1H, C2-H), 8.21 (t, 2H, C10-H), 8.60 (d, 1H, C5-H), 8.67 (t, 1H, C11-H), 9.09 (d, 2H, C9-H), 11.55 (s, 1H, NH).  $^{13}C$  NMR (125 MHz, DMSO- $d_6$ ),  $\delta$  (ppm): 12.76 (C7), 62.35 (C8), 120.66 (C2),

124.76 (C4), 128.01 (C10), 137.09 (C3), 146.67 (C11), 146.89 (C9), 149.15 (C5), 150.94 (C6), 154.99 (C1), 168.19 (C12).

**Synthesis of complex  $[ZnL^4(N_3)_2]$  (4):**  $Zn^{II}$  complex 4 was synthesised by the reaction of  $HL^4Cl$  (87 mg, 0.30 mmol) and  $Zn(BF_4)_2 \cdot 6H_2O$  (104 mg, 0.30 mmol) in a solvent mixture of MeOH/ $CH_3CN/H_2O$  (20/10/5 mL, Scheme 4b). After complete dissolution of  $Zn(BF_4)_2 \cdot 6H_2O$  in reaction mixture,  $NaN_3$  (78 mg, 1.20 mmol) was added. The mixture was refluxed for 2 h. After slow evaporation of solvent at room temperature for one day, yellow crystals were obtained. Yield: 87 mg (67%). Elemental analysis calcd. for  $C_{14}H_{14}N_{10}OZn$ : C 41.65%, H 3.49%, N 34.69%; found: C 41.45%, H 3.51%, N 34.61%. IR (ATR,  $cm^{-1}$ ): 3390 (w), 3137 (w), 3092 (w), 2997 (w), 2937 (w), 2079 (s), 2055 (s), 1630 (w), 1595 (w), 1569 (w), 1538 (m), 1485 (w), 1462 (m), 1440 (w), 1362 (m), 1320 (w), 1261 (w), 1208 (w), 1189 (w), 1153 (w), 1091 (w), 1021 (w), 785 (w), 724 (w), 677 (w), 634 (w).  $^1H$  NMR (400 MHz, DMSO- $d_6$ ),  $\delta$  (ppm): 2.31 (s, 3H, C7-H), 5.48 (s, 2H, C8-H), 7.62 (dd, 1H, C4-H), 7.89 (d, 1H, C2-H), 8.08 (t, 1H, C3-H), 8.13 (t, 2H, C10-H), 8.43 (d, 1H, C5-H), 8.61 (t, 1H, C11-H), 9.03 (d, 2H, C9-H).  $^{13}C$  NMR (125 MHz, DMSO- $d_6$ ),  $\delta$  (ppm): 12.74 (C7), 62.77 (C8), 123.26 (C2), 126.1 (C4), 127.77 (C10), 140.62 (C3), 146.21 (C11), 146.53 (C9), 148.79 (C5), 149.32 (C1), 161.39 (C6), 172.52 (C12).

**Synthesis of ligand  $HL^5Cl$ :** The ligand  $HL^5Cl$  was synthesised by the reaction of 2-quinolinecarboxaldehyde and Girard's T reagent according to the previously described method.<sup>[61]</sup> Elemental analysis calcd. for  $C_{15}H_{19}ClN_4O$ : C 58.73%, H 6.24%, N 18.26%; found: C 58.96%, H 6.13%, N 18.02%. IR (ATR,  $cm^{-1}$ ): 3414 (m), 3062 (m), 2970 (m), 2939 (m), 2831 (m), 1699 (s), 1595 (m), 1562 (w), 1497 (m), 1414 (m), 1379 (w), 1340 (w), 1301 (m), 1230 (m), 1135 (m), 989 (w), 950 (w), 916 (w), 868 (w), 832 (w), 758 (m), 656 (w), 633 (w), 533 (w).  $^1H$  NMR (400 MHz,  $CD_3OD$ ),  $\delta$  (ppm) 3.47 (s, 9H, C12-H), 4.94 (s, 2H, C11-H), 8.17 (s, 1H, C9-H), 8.18 (d, 1H, 3J $C_3$ -H/C4-H = 10 Hz, C3-H), 8.36 (d, 1H, C4-H), 7.94 (d, 1H, C5-H), 7.62 (t, 1H, C6-H), 7.78 (t, 1H, C7-H), 8.03 (d, 1H, C8-H).

**Synthesis of complex 5:**  $Zn^{II}$  complex 5 was synthesised by the reaction of  $HL^5Cl$ ,  $Zn(BF_4)_2 \cdot 6H_2O$ , and  $NaN_3$  according to the previously described method.<sup>[25]</sup> Elemental analysis calcd. for  $C_{15}H_{18}N_{10}OZn$ : C 42.92%, H 4.32%, N 33.37%; found: C 43.03%, H 4.56%, N 33.35%. IR (ATR,  $cm^{-1}$ ): 3310 (w), 3027 (w), 2939 (w), 2817 (w), 2169 (w), 2067 (s), 1923 (w), 1748 (w), 1645 (w), 1612 (w), 1566 (s), 1535 (s), 1398 (m), 1344 (w), 1300 (s), 1232 (w), 1125 (w), 1086 (s), 1032 (w), 972 (w), 925 (m), 873 (w), 833 (w), 785 (w), 757 (m), 632 (w), 589 (w).  $^1H$  NMR (400 MHz, DMSO- $d_6$ ),  $\delta$  (ppm) 3.28 (s, 9H, C12-H), 4.17 (s, 2H, C11-H), 8.38 (s, 1H, C9-H), 7.71 (d, 1H, C3-H), 8.09 (d, 1H, C4-H), 8.70 (d, 1H, C5-H), 7.91 (m, 1H, C6-H), 7.91 (m, 1H, C7-H), 8.70 (d, 1H, C8-H).

**Synthesis of complex 6:**  $Zn^{II}$  complex 6 was synthesised by the reaction of  $HL^5Cl$ ,  $Zn(BF_4)_2 \cdot 6H_2O$ , and NaOCN according to the previously described method.<sup>[25]</sup> Elemental Anal. Calcd for  $C_{17}H_{18}N_6O_3Zn$ : C 48.64%, H 4.32%, N 20.02%; found: C 48.73%, H 4.47%, N 19.98%. IR (ATR,  $cm^{-1}$ ): 3536 (w), 3063 (w), 2966 (w), 2203 (s), 1611 (w), 1563 (m), 1530 (s), 1482 (w), 1400 (w), 1343 (w), 1305 (w), 1242 (w), 1203 (w), 1124 (w), 1080 (w), 1026 (w), 995 (w), 972 (w), 931 (w), 830 (w), 807 (w), 785 (w), 752 (w), 629 (w).  $^1H$  NMR (400 MHz, DMSO- $d_6$ ),  $\delta$  (ppm) 3.27 (s, 9H, C12-H), 4.15 (s, 2H, C11-H), 8.34 (s, 1H, C9-H), 7.71 (d, 1H, C3-H), 8.09 (d, 1H, C4-H), 8.66 (d, 1H, C5-H), 7.91 (m, 1H, C6-H), 7.91 (m, 1H, C7-H), 8.66 (d, 1H, C8-H).

### X-Ray Crystallography

Crystal data and refinement parameters of compounds 3 and 4 are listed in Table 4. Single crystal X-ray diffraction data were collected at room temperature on an Agilent SuperNova dual-source



Table 4. Crystal data and structure refinement details for 3 and 4.		
	3	4
formula	C <sub>6</sub> H <sub>7</sub> N <sub>2</sub> S <sub>2</sub> Zn	C <sub>14</sub> H <sub>14</sub> N <sub>10</sub> OZn
Fw (g mol <sup>-1</sup> )	306.68	403.72
crystal size (mm)	0.50×0.30×0.10	0.50×0.10×0.10
crystal color	yellow	colourless
crystal system	monoclinic	monoclinic
space group	<i>P</i> 2 <sub>1</sub> / <i>c</i>	<i>P</i> 2 <sub>1</sub> / <i>c</i>
<i>a</i> (Å)	7.4254(3)	12.3417(5)
<i>b</i> (Å)	18.6798(8)	8.9990(5)
<i>c</i> (Å)	7.9925(4)	15.3451(6)
$\beta$ (°)	100.930(4)	101.169(4)
<i>V</i> (Å <sup>3</sup> )	1088.49(9)	1671.99(13)
<i>Z</i>	4	4
calcd density (g cm <sup>-3</sup> )	1.871	1.604
<i>F</i> (000)	616	824
no. of collected reflns	10146	15739
no. of independent reflns	2503	3828
<i>R</i> <sub>int</sub>	0.0349	0.0320
no. of reflns observed	2190	3007
no. parameters	152	236
<i>R</i> [ <i>I</i> > 2σ ( <i>I</i> )] <sup>[a]</sup>	0.0289	0.0331
<i>wR</i> <sub>2</sub> (all data) <sup>[b]</sup>	0.0720	0.0823
Goof, <i>S</i> <sup>[c]</sup>	1.089	1.052
maximum/minimum residual electron density (e Å <sup>-3</sup> )	+0.33/−0.54	+0.38/−0.30

[a]  $R = \sum ||F_o| - |F_c|| / \sum |F_o|$ . [b]  $wR_2 = \{\sum [w(F_o^2 - F_c^2)^2] / \sum [w(F_o^2)^2]\}^{1/2}$ . [c]  $S = \{\sum [(F_o^2 - F_c^2)^2] / (n/p)\}^{1/2}$  where *n* is the number of reflections and *p* is the total number of parameters refined.

diffractometer with an Atlas detector equipped with mirror-monochromated Mo-K<sub>α</sub> radiation ( $\lambda = 0.71073$  Å).

Data processing was performed with CrysAlis PRO.<sup>[63]</sup> The structures were solved by direct methods (SHELXS-2013/1)<sup>[64]</sup> and refined by a full-matrix least-squares procedure based on *F*<sup>2</sup> using SHELXL-2018/3.<sup>[65]</sup> All non-hydrogen atoms were refined anisotropically. The nitrogen bonded hydrogen atoms were located in the difference map and refined with the distance restraints (DFIX) with *d*(N–H) = 0.86 Å and with *U*<sub>iso</sub>(H) = 1.2*U*<sub>eq</sub>(N). All other hydrogen atoms were included in the model at geometrically calculated positions and refined using a riding model. Deposition Numbers 2244671 (for 3), 2244672 (for 4) contain the supplementary crystallographic data for this paper. These data are provided free of charge by the joint Cambridge Crystallographic Data Centre and Fachinformationszentrum Karlsruhe Access Structures service.

### Catalysis General Procedure

All manipulations were performed under an Ar atmosphere using standard Schlenk techniques. To avoid undesired solidification of the reaction mixtures, a few substrates required the use of a solvent and, in this case, a small amount of dry toluene was added. In a J Young tube which was flame dried (×3) and equipped with a stirring bar, were added 5 mol% of the catalyst and 0.5 mmol of

the amine. The mixture was stirred until the solid was partially dissolved. Then, 0.5 mmol of the alkyne and 0.5 mmol of the ketone were added, following the addition of dry toluene (if so required) and the drying agent in the pressure tube. The reaction mixture was stirred for 16 hours at 130 °C in an oil bath. After cooling to room temperature, ethyl acetate was added and the reaction mixture was filtered through a pad of celite. The solvent was removed under reduced pressure and was subjected to column chromatography, using petroleum ether/ethyl acetate to afford the pure propargylamine substrates. All products were characterised by <sup>1</sup>H-NMR and the results are in full agreement with the data reported in the literature.

### Characterisation data of the propargylamine products

**1-(1-(phenylethynyl)cyclohexyl)piperidine (4a):** Obtained as a yellow oil in 85% isolated yield (112 mg, 0.41 mmol). <sup>1</sup>H-NMR (200 MHz, CDCl<sub>3</sub>)  $\delta$  7.45–7.40 (m, 2H), 7.35–7.23 (m, 3H), 2.66 (t, *J* = 5.4 Hz, 4H), 2.10 (d, *J* = 11.4 Hz, 2H), 1.68–1.37 (m, 14H, overlapping peaks).<sup>[66]</sup>

**4-(1-(phenylethynyl)cyclohexyl)morpholine (4b):** Obtained as an orange oil in 67% isolated yield (91 mg, 0.33 mmol). <sup>1</sup>H-NMR (400 MHz, CDCl<sub>3</sub>)  $\delta$  7.43 (dt, *J* = 6.0, 3.8 Hz, 2H), 7.29 (q, *J* = 3.3, 2.3 Hz, 3H), 3.77 (t, *J* = 4.8 Hz, 4H), 2.73 (t, *J* = 4.7 Hz, 4H), 2.07–2.00 (m, 2H), 1.73 (dt, *J* = 10.3, 5.0 Hz, 2H), 1.63 (dd, *J* = 12.6, 3.1 Hz, 2H), 1.56–1.47 (m, 2H), 1.28 (s, 1H).<sup>[35]</sup>

**N-octyl-1-(phenylethynyl)cyclohexan-1-amine (4c):** Obtained as a yellow oil in 42% isolated yield (64 mg, 0.20 mmol). <sup>1</sup>H-NMR (400 MHz, CDCl<sub>3</sub>)  $\delta$  7.42 (dd, *J* = 6.7, 3.1 Hz, 2H), 7.33–7.23 (m, 3H), 2.79 (t, *J* = 7.1 Hz, 2H), 1.94 (d, *J* = 11.6 Hz, 2H), 1.74–1.07 (m, 20H), 0.88 (m, 3H).<sup>[38]</sup>

**1-(phenylethynyl)-*N,N*-dipropylcyclohexan-1-amine (4d):** Obtained as an orange oil in 40% isolated yield (57 mg, 0.20 mmol). <sup>1</sup>H-NMR (200 MHz, CDCl<sub>3</sub>)  $\delta$  7.47–7.37 (m, 2H), 7.33–7.24 (m, 3H), 2.62 (t, *J* = 7.8 Hz, 4H), 2.05 (d, *J* = 11.8 Hz, 2H), 1.76–1.42 (m, 12H), 0.87 (t, *J* = 7.3 Hz, 6H).<sup>[38]</sup>

**1-(1-(*p*-tolylethynyl)cyclohexyl)pyrrolidine (4e):** Obtained as a yellow oil in 50% isolated yield (67 mg, 0.49 mmol). <sup>1</sup>H-NMR (400 MHz, CDCl<sub>3</sub>)  $\delta$  7.32 (d, *J* = 7.8 Hz, 2H), 7.11 (d, *J* = 7.8 Hz, 2H), 2.90 (d, *J* = 6.3 Hz, 4H), 2.35 (s, 3H), 2.04–1.98 (m, 2H), 1.84–1.81 (m, 4H), 1.70–1.60 (m, 8H).<sup>[38]</sup>

**1-(1-(4-chlorophenyl)ethynyl)cyclohexyl)pyrrolidine (4f):** Obtained as an orange oil in 38% isolated yield (54 mg, 0.20 mmol). <sup>1</sup>H-NMR (200 MHz, CDCl<sub>3</sub>)  $\delta$  7.40–7.31 (m, 2H), 7.22–7.18 (m, 2H), 2.76–2.67 (m, 4H), 2.00–1.88 (m, 2H), 1.81–1.38 (m, 12H).<sup>[38]</sup>

**1-(1-(4-methoxyphenyl)ethynyl)cyclohexyl)piperidine (4g):** Obtained as an orange oil in 96% isolated yield (142 mg, 0.48 mmol). <sup>1</sup>H-NMR (400 MHz, CDCl<sub>3</sub>)  $\delta$  7.37 (d, *J* = 8.6 Hz, 2H), 6.83 (d, *J* = 8.5 Hz, 2H), 3.81 (s, 3H), 2.73 (s, 4H), 2.10 (d, *J* = 11.8 Hz, 2H), 1.78–1.37 (m, 15H, overlapping peaks).<sup>[67]</sup>

**1-(1-(oct-1-yn-1-yl)cyclohexyl)pyrrolidine (4h):** Obtained as a yellow oil in 43% isolated yield (62 mg, 0.23 mmol). <sup>1</sup>H-NMR (400 MHz, CDCl<sub>3</sub>)  $\delta$  2.78 (d, *J* = 6.1 Hz, 4H), 2.23 (t, *J* = 6.8 Hz, 2H), 1.89 (d, *J* = 11.6 Hz, 2H), 1.78 (s, 4H), 1.67–1.43 (m, 14H), 0.91 (dt, *J* = 12.8, 6.8 Hz, 7H).<sup>[68]</sup>

**1-(3-ethyl-1-phenylpent-1-yn-3-yl)pyrrolidine (4i):** Obtained as a yellow oil in 75% isolated yield (94 mg, 0.38 mmol). <sup>1</sup>H-NMR (400 MHz, CDCl<sub>3</sub>)  $\delta$  7.45–7.38 (m, 2H), 7.28 (d, *J* = 5.4 Hz, 3H), 2.76 (s, 4H), 1.76 (m, 8H), 0.96 (t, *J* = 7.5 Hz, 6H).<sup>[37]</sup>

## Computational Details

All DFT calculations were done with the ADF<sup>[69,70]</sup> engine in Amsterdam Modeling Suite (version 2022.102).<sup>[71]</sup> Relativistic effects were accounted for by the scalar-relativistic Zeroth-Order Regular Approximation (ZORA).<sup>[71–74]</sup> The positions of hydrogen atoms were optimised with the Fast Inertial Relaxation Engine<sup>[75]</sup> based optimizer in Cartesian coordinates. All other atoms were kept fixed at the positions from X-ray determined geometries of Zn<sup>II</sup> complexes 1–6. For optimisation of hydrogen atoms, general gradient approximation consisting of Becke's exchange<sup>[76]</sup> and Perdew's correlation<sup>[77]</sup> with Grimme's fourth generation dispersion energy corrections,<sup>[78]</sup> (BP86-D4) was used. The all-electron double-zeta Slater-type orbitals plus one polarisation function (DZP) basis set was used. Global reactivity descriptors in the framework of Conceptual DFT were calculated.<sup>[59]</sup> The finite difference linearisation (FDL) and frontier molecular orbital approximation (FMO) were used to estimate descriptors.<sup>[59]</sup> For calculations of energies of complexes with one electron more or less, as needed for the FDL approach, unrestricted formalism was used. Range-separated hybrid CAM-B3LYP<sup>[79]</sup> functional, all-electron triple-zeta Slater-type orbitals plus one polarisation function (TZP) basis set and an increased numerical grid ("Becke grid Quality good" in ADF) were used for Conceptual DFT calculations. The LibXC library<sup>[80]</sup> was used for calculations employing CAM-B3LYP functional.

## Supporting Information

See Supporting Information for the structural parameters, the selected bond lengths and angles and the raw data of the IR and NMR spectra for complexes 3 and 4 and their corresponding ligands (HL<sup>3</sup> and HL<sup>4</sup>Cl, respectively).

## Acknowledgements

The publication of the article in OA mode was financially supported by HEAL-Link. The research project was supported by the Hellenic Foundation for Research and Innovation (H. F. R. I.) under the "1st Call for H. F. R. I. Research Projects to support Faculty Members & Researchers and the procurement of high-cost research equipment grant" (Project Number: 16). Moreover, this research has been financially supported by the Ministry of Science, Technological Development and Innovation of Republic of Serbia, contract numbers: 451-03-47/2023-01/200026 and 451-03-47/2023-01/200168, as well as by the Science Fund of the Republic of Serbia, #7750288, Tailoring Molecular Magnets and Catalysts Based on Transition Metal Complexes – TMMagCat, and by the Slovenian Research Agency (ARRS), grant number P1-0175. We thank the EN-FIST Centre of Excellence, Ljubljana, Slovenia, for the use of the SuperNova diffractometer.

## Conflict of Interests

The authors declare no conflict of interest.

## Data Availability Statement

The data that support the findings of this study are available from the corresponding author upon reasonable request.

**Keywords:** Schiff bases · XRD · ketone-amine-alkyne coupling reaction · Density Functional Theory

- [1] R. N. Patel, Y. Singh, Y. P. Singh, R. J. Butcher, A. Kamal, I. P. Tripathi, *Polyhedron* **2016**, *117*, 20–34.
- [2] S. Mondal, B. Pakhira, A. J. Blake, M. G. B. Drew, S. K. Chattopadhyay, *Polyhedron* **2016**, *117*, 327–337.
- [3] M. de Gracia Retamosa, E. Matador, D. Monge, J. M. Lassaletta, R. Fernández, *Chem. A Eur. J.* **2016**, *22*, 13430–13445.
- [4] R. S. Nair, M. Kuriakose, V. Somasundaram, V. Shenoj, M. R. P. Kurup, P. Srinivas, *Life Sci.* **2014**, *116*, 90–97.
- [5] H. Abd El-Wahab, M. Abd El-Fattah, A. H. Ahmed, A. A. Elhenawy, N. A. Alian, *J. Organomet. Chem.* **2015**, *791*, 99–106.
- [6] G. Li, Q. Zhang, S. Yang, M. Zhu, Y. Fu, Z. Liu, N. Xing, L. Shi, *J. Coord. Chem.* **2022**, *75*, 1416–1433.
- [7] P. Khatkar, S. Asija, N. Singh, *J. Serb. Chem. Soc.* **2017**, *82*, 13–23.
- [8] S. Koner, S. Saha, T. Mallah, K.-I. Okamoto, *Inorg. Chem.* **2004**, *43*, 840–842.
- [9] E. B. Seena, N. Mathew, M. Kuriakose, M. R. P. Kurup, *Polyhedron* **2008**, *27*, 1455–1462.
- [10] J. Chakraborty, S. Thakurta, G. Pilet, D. Luneau, S. Mitra, *Polyhedron* **2009**, *28*, 819–825.
- [11] A. M. Greenaway, C. J. O'Connor, A. Schrock, E. Sinn, *Inorg. Chem.* **1979**, *18*, 2692–2695.
- [12] S. Biswas, G. P. A. Yap, K. Dey, *Polyhedron* **2009**, *28*, 3094–3100.
- [13] F. A. Afkhami, A. A. Khandar, G. Mahmoudi, M. Amini, E. Molins, P. Garczarek, J. Lipkowski, J. M. White, A. M. Kirillov, *Inorg. Chim. Acta* **2017**, *458*, 68–76.
- [14] A. A. Recio Despaigne, J. G. Da Silva, A. C. M. Do Carmo, O. E. Piro, E. E. Castellano, H. Beraldo, *J. Mol. Struct.* **2009**, *920*, 97–102.
- [15] Z. Xu, X. Mao, P. Zhang, H. Li, Y. Wang, M. Liu, L. Jia, *J. Mol. Struct.* **2017**, *1128*, 665–673.
- [16] M. Bakir, R. R. Conry, O. Green, W. H. Mulder, *J. Coord. Chem.* **2008**, *61*, 3066–3079.
- [17] F. A. Afkhami, A. A. Khandar, G. Mahmoudi, W. Maniukiewicz, J. Lipkowski, J. M. White, R. Waterman, S. García-Granda, E. Zangrando, A. Bauzá, A. Frontera, *CrystEngComm* **2016**, *18*, 4587–4596.
- [18] X. J. Hong, Q. G. Zhan, Z. P. Huang, Y. Q. Du, L. M. Wei, T. Li, Z. P. Zheng, Y. P. Cai, *Inorg. Chem. Commun.* **2014**, *44*, 53–57.
- [19] F. A. Afkhami, A. A. Khandar, G. Mahmoudi, W. Maniukiewicz, A. V. Gurbanov, F. I. Zubkov, O. Şahin, O. Z. Yesilel, A. Frontera, *CrystEngComm* **2017**, *19*, 1389–1399.
- [20] K. Anđelković, A. Pevec, S. Grubišić, I. Turel, B. Čobeljić, M. R. Milenković, T. Keškić, D. Radanović, *J. Mol. Struct.* **2018**, *1162*, 63–70.
- [21] S. Dasgupta, S. Karim, S. Banerjee, M. Saha, K. Das Saha, D. Das, *Dalton Trans.* **2020**, *49*, 1232–1240.
- [22] S. O. Malinkin, L. Penkova, Y. S. Moroz, M. Haukka, A. Maciag, E. Gumienna-Kontecka, V. A. Pavlenko, S. Pavlova, E. Nordlander, I. O. Fritsky, *Eur. J. Inorg. Chem.* **2012**, *2012*, 1639–1649.
- [23] D. Kovala-Demertzi, P. N. Yadav, J. Wiecek, S. Skoulika, T. Varadinova, M. A. Demertzi, *J. Inorg. Biochem.* **2006**, *100*, 1558–1567.
- [24] N. Stevanović, P. P. Mazzeo, A. Bacchi, I. Z. Matić, M. Đorđić Crnogorac, T. Stanojković, M. Vujčić, I. Novaković, D. Radanović, M. Šumar-Ristović, D. Sladić, B. Čobeljić, K. Anđelković, *J. Biol. Inorg. Chem.* **2021**, *26*, 863–880.
- [25] M. Č. Romanović, B. Čobeljić, A. Pevec, I. Turel, K. Anđelković, M. M. R. Milenković, D. Radanović, S. Belošević, M. M. R. Milenković, *J. Coord. Chem.* **2017**, *70*, 2425–2435.
- [26] A. E. Stacy, D. Palanimuthu, P. V. Bernhardt, D. S. Kalinowski, P. J. Jansson, D. R. Richardson, *J. Med. Chem.* **2016**, *59*, 4965–4984.
- [27] N. Stevanović, M. Zlatar, I. Novaković, A. Pevec, D. Radanović, I. Z. Matić, M. Đorđić Crnogorac, T. Stanojković, M. Vujčić, M. Gruden, D. Sladić, K. Anđelković, I. Turel, B. Čobeljić, *Dalton Trans.* **2022**, *51*, 185–196.
- [28] N. C. Kasuga, Y. Hara, C. Koumo, K. Sekino, K. Nomiya, *Acta Crystallogr. Sect. C* **1999**, *55*, 1264–1267.
- [29] E. Viñuelas-Zahinos, F. Luna-Giles, P. Torres-García, M. C. Fernández-Calderón, *Eur. J. Med. Chem.* **2011**, *46*, 150–159.

- [30] T. T. Adejumo, N. V. Tzouras, L. P. Zorba, D. Radanović, A. Pevec, S. Grubišić, D. Mitić, K. K. Anđelković, G. C. Vougioukalakis, B. Čobeljić, I. Turel, *Molecules* **2020**, *25*, 4043.
- [31] S. P. Cronin, A. Al Mamun, M. J. Toda, M. S. Mashuta, Y. Losovj, P. M. Kozłowski, R. M. Buchanan, C. A. Grapperhaus, *Inorg. Chem.* **2019**, *58*, 12986–12997.
- [32] K. Lauder, A. Toscani, N. Scalacci, D. Castagnolo, *Chem. Rev.* **2017**, *117*, 14091–14200.
- [33] L. P. Zorba, G. C. Vougioukalakis, *Coord. Chem. Rev.* **2021**, *429*, 213603.
- [34] O. P. Pereshivko, V. A. Peshkov, E. V. Van der Eycken, *Org. Lett.* **2010**, *12*, 2638–2641.
- [35] M. Cheng, Q. Zhang, X.-Y. Hu, B.-G. Li, J.-X. Ji, A. S. C. Chan, *Adv. Synth. Catal.* **2011**, *353*, 1274–1278.
- [36] C. J. Pierce, M. Nguyen, C. H. Larsen, *Angew. Chem. Int. Ed.* **2012**, *51*, 12289–12292.
- [37] N. V. Tzouras, S. P. Neofotistos, G. C. Vougioukalakis, *ACS Omega* **2019**, *4*, 10279–10292.
- [38] S. P. Neofotistos, N. V. Tzouras, M. Pauze, E. Gómez-Bengoia, G. C. Vougioukalakis, *Adv. Synth. Catal.* **2020**, *362*, 3872–3885.
- [39] L. Bresolin, R. A. Burlow, M. Hörner, E. Bermejo, A. Castiñeras, *Polyhedron* **1997**, *16*, 3947–3951.
- [40] E. N. Nfor, W. Liu, J.-L. Zuo, X.-Z. You, O. E. Offiong, *Acta Crystallogr. Sect. C* **2006**, *62*, m211–m213.
- [41] E. Bermejo, A. Castiñeras, I. García-Santos, D. X. West, *Z. Anorg. Allg. Chem.* **2005**, *631*, 2011–2019.
- [42] A. H. Mirza, M. H. S. A. Hamid, S. Aripin, M. R. Karim, M. Arifuzzaman, M. A. Ali, P. V. Bernhardt, *Polyhedron* **2014**, *74*, 16–23.
- [43] E. Bermejo, A. Castiñeras, I. García-Santos, D. X. West, *Z. Anorg. Allg. Chem.* **2004**, *630*, 1096–1109.
- [44] C. de Q. O. Cavalcante, D. da S. Arcanjo, G. G. da Silva, D. M. de Oliveira, C. C. Gatto, *New J. Chem.* **2019**, *43*, 11209–11221.
- [45] I. García, E. Bermejo, A. K. El Sawaf, A. Castiñeras, D. X. West, *Polyhedron* **2002**, *21*, 729–737.
- [46] N. Arefyeva CCDC 1435302.
- [47] B. Čobeljić, A. Pevec, S. Stepanović, M. R. Milenković, I. Turel, M. Gruden, D. Radanović, K. Anđelković, *Struct. Chem.* **2018**, *29*, 1797–1806.
- [48] A. Sy, M. Dieng, I. E. Thiam, M. Gaye, P. Retailleau, *Acta Crystallogr. Sect. E* **2013**, *69*, m108–m108.
- [49] A. A. R. Despaigne, J. G. Da Silva, A. C. M. do Carmo, O. E. Piro, E. E. Castellano, H. Beraldo, *Inorg. Chim. Acta* **2009**, *362*, 2117–2122.
- [50] F. A. Afkhami, G. Mahmoudi, A. A. Khandar, J. M. White, W. Maniukiewicz, *J. Mol. Struct.* **2019**, *1197*, 555–563.
- [51] H. Yu, S. Guo, J.-Y. Cheng, G. Jiang, Z. Li, W. Zhai, A. Li, Y. Jiang, Z. You, *J. Coord. Chem.* **2018**, *71*, 4164–4179.
- [52] L. J. Farrugia, *J. Appl. Crystallogr.* **2012**, *45*, 849–854.
- [53] C. R. Groom, I. J. Bruno, M. P. Lightfoot, S. C. Ward, *Acta Crystallogr. Sect. B* **2016**, *72*, 171–179.
- [54] A. L. Spek, *J. Appl. Crystallogr.* **2003**, *36*, 7–13.
- [55] G. Liu, D. A. Cogan, T. D. Owens, T. P. Tang, J. A. Ellman, *J. Org. Chem.* **1999**, *64*, 1278–1284.
- [56] L. P. Zorba, E. Egaña, E. Gómez-Bengoia, G. C. Vougioukalakis, *ACS Omega* **2021**, *6*, 23329–23346.
- [57] H. Chermette, *J. Comput. Chem.* **1999**, *20*, 129–154.
- [58] P. Geerlings, F. De Proft, W. Langenaeker, *Chem. Rev.* **2003**, *103*, 1793–1874.
- [59] J. Dostanić, D. Lončarević, M. Zlatar, F. Vlahović, D. M. Jovanović, *J. Hazard. Mater.* **2016**, *316*, 26–33.
- [60] G. Hoffmann, V. Tognetti, L. Joubert, *J. Mol. Model.* **2018**, *24*, 281.
- [61] B. Čobeljić, I. Turel, A. Pevec, Z. Jagličić, D. Radanović, K. Anđelković, M. R. Milenković, *Polyhedron* **2018**, *155*, 425–432.
- [62] M. Č. Romanović, B. R. Čobeljić, A. Pevec, I. Turel, V. Spasojević, A. A. Tsaturyan, I. N. Shcherbakov, K. K. Anđelković, M. M. R. Milenković, D. Radanović, M. M. R. Milenković, *Polyhedron* **2017**, *128*, 30–37.
- [63] Agilent (2014) CrysAlis Pro.
- [64] G. M. Sheldrick, *Acta Crystallogr. Sect. A* **2008**, *64*, 112–122.
- [65] G. M. Sheldrick, *Acta Crystallogr. Sect. A* **2015**, *71*, 3–8.
- [66] C. J. Pierce, C. H. Larsen, *Green Chem.* **2012**, *14*, 2672–2676.
- [67] A. P. Shah, A. S. Sharma, S. Jain, N. G. Shimpi, *N. J. Chem.* **2018**, *42*, 8724–8737.
- [68] F. Schlimpen, C. Plaças, E. Starck, V. Bénétteau, P. Pale, S. Chassaing, *J. Org. Chem.* **2021**, *86*(23), 16593–16613.
- [69] G. te Velde, F. M. Bickelhaupt, E. J. Baerends, C. Fonseca Guerra, S. J. A. van Gisbergen, J. G. Snijders, T. Ziegler, *J. Comput. Chem.* **2001**, *22*, 931–967.
- [70] E. J. Baerends, T. Ziegler, A. J. Atkins, J. Autschbach, D. Bashford, O. Baseggio, A. Bérces, F. M. Bickelhaupt, C. Bo, P. M. Boerrigter, L. Cavallo, C. Daul, D. P. Chong, D. v Chulhai, L. Deng, R. M. Dickson, J. M. Dieterich, D. E. Ellis, M. van Faassen, A. Ghysels, A. Giammona, S. J. A. van Gisbergen, A. Goez, A. W. Götz, S. Gusarov, F. E. Harris, P. van den Hoek, Z. Hu, C. R. Jacob, H. Jacobsen, L. Jensen, L. Joubert, J. W. Kaminski, G. van Kessel, C. König, F. Kootstra, A. ADF 2022.1, SCM, Theoretical Chemistry, Vrije Universiteit, Amsterdam, The Netherlands.
- [71] T. N. R. Rüger, M. Franchini, T. Trnka, A. Yakovlev, E. van Lenthe, P. Philipsen, T. van Vuren, B. Klumpers, T. Soini, AMS 2022.1, SCM, Theoretical Chemistry, Vrije Universiteit, Amsterdam.
- [72] E. van Lenthe, E. J. Baerends, J. G. Snijders, *J. Chem. Phys.* **1993**, *99*, 4597–4610.
- [73] E. van Lenthe, E. J. Baerends, J. G. Snijders, *J. Chem. Phys.* **1994**, *101*, 9783–9792.
- [74] C. van Wüllen, *J. Chem. Phys.* **1998**, *109*, 392–399.
- [75] E. Bitzek, P. Koskinen, F. Gähler, M. Moseler, P. Gumbusch, *Phys. Rev. Lett.* **2006**, *97*, 170201.
- [76] A. D. Becke, *Phys. Rev. A* **1988**, *38*, 3098–3100.
- [77] J. P. Perdew, *Phys. Rev. B* **1986**, *33*, 8822–8824.
- [78] E. Caldeweyher, S. Ehlert, A. Hansen, H. Neugebauer, S. Spicher, C. Bannwarth, S. Grimme, *J. Chem. Phys.* **2019**, *150*, 154122.
- [79] T. Yanai, D. P. Tew, N. C. Handy, *Chem. Phys. Lett.* **2004**, *393*, 51–57.
- [80] M. A. L. Marques, M. J. T. Oliveira, T. Burnus, *Comput. Phys. Commun.* **2012**, *183*, 2272–2281.

Manuscript received: April 3, 2023  
Revised manuscript received: July 21, 2023  
Accepted manuscript online: August 26, 2023  
Version of record online: September 28, 2023